

DiffusionFace: Towards a Comprehensive Dataset for Diffusion-Based Face Forgery Analysis

Zhongxi Chen, Ke Sun, Ziyin Zhou, Xianming Lin, Xiaoshuai Sun, Liujuan Cao, Rongrong Ji
Key Laboratory of Multimedia Trusted Perception and Efficient Computing,
Ministry of Education of China, Xiamen University, China

Abstract

*The rapid progress in deep learning has given rise to hyper-realistic facial forgery methods, leading to concerns related to misinformation and security risks. Existing face forgery datasets have limitations in generating high-quality facial images and addressing the challenges posed by evolving generative techniques. To combat this, we present **DiffusionFace**, the first diffusion-based face forgery dataset, covering various forgery categories, including unconditional and Text Guide facial image generation, Img2Img, Inpaint, and Diffusion-based facial exchange algorithms. Our DiffusionFace dataset stands out with its extensive collection of 11 diffusion models and the high-quality of the generated images, providing essential metadata and a real-world internet-sourced forgery facial image dataset for evaluation. Additionally, we provide an in-depth analysis of the data and introduce practical evaluation protocols to rigorously assess discriminative models' effectiveness in detecting counterfeit facial images, aiming to enhance security in facial image authentication processes. The dataset is available for download at <https://github.com/Rapisurazurite/DiffFace>.*

1. Introduction

In recent years, the field of facial forgery generation has witnessed significant advancements, predominantly fueled by strides in deep learning. These developments have facilitated the creation of hyper-realistic counterfeit facial images and videos, leading to a surge in their convincingness. The proliferation of such technology, however, has raised substantial concerns. It has opened avenues for misuse, such as spreading misinformation, maligning public figures, or undermining identity verification systems, potentially leading to dire consequences in political, societal, and security domains.

Currently, there is an abundance of publicly accessible DeepFake datasets utilized for research purposes,

such as FaceForensics++ [33], ForgeyNet [13], and Celeb-DF [20]. These datasets predominantly employ two types of facial generation techniques: Computer Graphics (CG) and learning-based methods. Representative examples of CG include NeuralTextures and MMReplacement. On the other hand, learning-based methods primarily utilize Auto-Encoders (AE) [17] and Generative Adversarial Networks (GAN) [12], with widely-known applications like FaceSwap [1], FakeApp [2], faceswap-GAN [3], and Deep-facelab [29]. With the advancement of deep learning, learning-based methods are increasingly garnering attention in the research community.

Recent progress in AI-generated content has seen diffusion models surpass AE and GAN-based methods in producing realistic images. Tools like Stable Diffusion [32] allow for the creation of forgery faces en masse, cheaply. However, this advancement also introduces new challenges for existing DeepFake detection models, which now struggle to cope with the subtle differences that diffusion techniques bring, such as the high-quality images and the reduction of artifacts and inconsistencies.

In response to the surge of forgeries produced by diffusion techniques [14, 35], several datasets targeting diffusion-generated images have emerged, including DE-FAKE [34], CIFAKE [5], GenImage [46], and DMD-LSUN [31]. However, they are not specifically tailored for facial forgeries. Facial forgery detection differs substantially from natural image analysis due to the need to identify intricate inconsistencies within facial features, the subtleties of human expression, and the complex interplay of lighting and texture that are unique to human faces. These nuances require specialized approaches to discern between authentic and manipulated images, where even minor deviations can be telltale signs of forgery.

To address these challenges, we present the first diffusion-based face forgery dataset, named DiffusionFace, which is designed to help develop advanced detection models capable of identifying forgery facial images created by diffusion methods. Our dataset extensively covers a variety of forgery categories, including Unconditional and Text-

Dataset Name	Public	Content	Diffusion Methods	Diffusion Categories	Paired Images	Paired Prompt	Real Images/Videos	Fake Images/Videos
Diffusion Image Dataset								
DE-FAKE [34]	×	General	4	T2I	✓	Text Prompt	192K	192K
CIFAKE [5]	✓	General	1	T2I	×	-	60K	60K
DMD-LSUN [31]	✓	Bedroom	5	UC	×	-	50K	500K
DiffusionForensics-LSUN [40]	✓	Bedroom	8	UC, T2I	×	-	42K	215K
DiffusionForensics-General [40]	✓	General	2	UC, T2I	×	-	50K	60K
CoCofake [4]	✓	General	1	T2I	✓	Text Prompt	123K	615K
GenImage [46]	✓	General	8	UC, T2I	×	-	1331K	1350K
Face Forgery Dataset								
UADFV [42]	×	Face	-	-	✓	-	241	252
FF++ [33]	✓	Face	-	-	✓	-	1K	1K
Celeb-DF [20]	✓	Face	-	-	✓	-	590	5639
DFFD [9]	✓	Face	-	-	✓	-	59K	240K
WDF [47]	✓	Face	-	-	✓	-	4K	4K
ForgeryNet [13]	✓	Face	-	-	✓	-	1438K	1458K
Ours	✓	Face	11	UC, T2I, I2I Inpaint, DiffSwap	✓	Text Prompt, Guide Image Inpaint Mask & Text Swapface id	30K	600K

Table 1. Dataset Content Comparison: Our dataset versus General Diffusion Image Datasets and Forgery Face Datasets. Here, UC stands for Unconditional image generation, T2I and I2I denote Text-guided image generation and Image-guided image Generation, respectively.

Guided facial image generation (T2I), as well as Img2Img (I2I), Inpainting, and advanced Diffusion-based facial exchange algorithms. This diverse range aims to establish a solid foundation for improving the precision and effectiveness of face forgery detection models in the evolving field of diffusion-based image generation.

Specifically, our proposed DiffusionFace leverages high-quality, richly annotated facial images from the Multi-Modal-CelebA-HQ [41] dataset to train a diverse set of diffusion-based forgery faces. We categorize the forgeries into two primary types: Unconditional Image Generation and Conditional Image Generation. Unconditional methods, which include popular diffusion models such as DDPM [14], DDIM [36], PNDM [22], P2 [8], and LDM [32], generate faces from random noise without any additional constraints. On the other hand, Conditional Image Generation harnesses extra information to guide the generation process. Specifically, we employ text prompts (text2Image), image constraints (image2image), context cues (Inpainting), and identity and expression parameters (DiffSwap [45]), utilizing models like Stable Diffusion 1.5, Stable Diffusion 2.1, and LDM to create the forgeries. Each image generated through conditional methods is associated with its respective caption, label, region mask, or targeted face ID. Table 1 presents a comparison of our DiffusionFace dataset with other forgery datasets. Notably, DiffusionFace includes 11 diffusion models, which is the most extensive

collection compared with other datasets. Our dataset also spans the widest variety of forgery categories, with five distinct types of generated content. Beyond this, Diffusion-Face offers the most comprehensive set of annotation categories available, which not only enables fine-grained classification for downstream tasks but also provides an enriched array of supervisory signals specifically beneficial for the training and evaluation of detection models.

Alongside the development and release of the Diffusion-Face dataset, our second key contribution is an in-depth analysis of the data. This analysis includes the introduction of practical testing protocols designed to challenge detection models in various scenarios: 1) a cross-model scenario that tests model robustness when the generative model type is unknown; 2) a cross-data scenario that assesses performance when the training data of the generative model is undisclosed; 3) a post-processing scenario that evaluates the detection of images modified by unidentified post-processing techniques.

2. Related Work

2.1. Existing DeepFake Datasets

The construction of DeepFake datasets for research on deep forgery detection methods entails substantial data collection and processing efforts. Presently, there exist publicly accessible and widely adopted DeepFake datasets, which

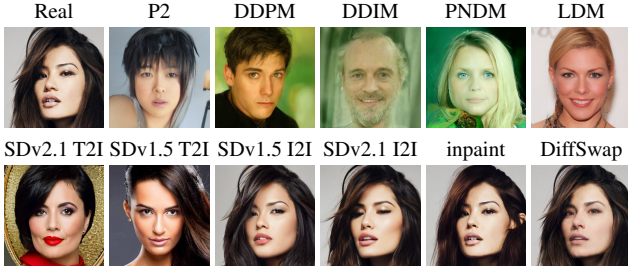


Figure 1. Examples of generated images. The first row illustrates Unconditional Image Generation, while the second row showcases Conditional Image Generation.

can be categorized into three generations based on their release timelines [13, 20], synthesis algorithms, and data scales. The first-generation datasets, such as UADFV [42] and DF-TIMIT [18], are relatively modest in scale. Second-generation datasets encompass Celeb-DF [20] and FaceForensics++ [33]. Among them, FaceForensics++ stands out as one of the most extensively utilized DeepFake detection datasets, featuring authentic and manipulated facial videos generated by multiple generative models. This dataset offers both original and manipulated videos with varying compression rates and resolutions, facilitating the assessment of deep forgery detection methods across diverse scenarios. The third-generation datasets, such as ForgeyNet [13], DPF [15], and DFDC [11], exhibit superior data scales and image quality. Nevertheless, these datasets predominantly rely on CG facial swapping techniques or GAN/AE, presenting challenges related to suboptimal image quality, thereby rendering them susceptible to detector detection due to prevalent visual artifacts.

2.2. Existing Diffusion Image Datasets

Addressing the surge of generated content online, initiatives like DE-FAKE have emerged, leveraging text-to-image models such as Stable Diffusion and Latent Diffusion to produce images, although access to DE-FAKE is restricted [34]. CIFAKE builds upon this by generating 6,000 images from CIFAR [19], using Stable Diffusion driven by random captions [5]. Further expanding the diversity, Ricker et al. [31] combines five diffusion models with GANs to create a significant corpus of 500,000 LSUN Bedroom [43] images. Similarly, DiffusionForensics [40] derives its dataset from LSUN Bedroom, adding a mix of unconditional and text-guided diffusion methods [40]. GenImage broadens the spectrum with a dataset for general diffusion model image detection, integrating outputs from eight different models [46]. CoCoFake [4] uniquely pairs its 600,000 generated images with original MSCOCO [21] counterparts, solely using the Text2Img approach from Stable Diffusion [4]. Yet, a specialized facial forgery detec-

tion dataset utilizing diffusion models is lacking. Our DiffusionFace dataset addresses this by offering a wide array of forgery methods and conditionally generated images that align one-to-one with their real counterparts, providing an essential tool for improving facial forgery detection.

3. DiffusionFace Dataset

3.1. Source Data

For the DiffusionFace dataset, we selected the high-resolution Multi-Modal-CelebA-HQ [41] dataset as our source data. Such a dataset contains 30,000 high-resolution facial images selected from CelebA [23]. Each image is accompanied by manually annotated semantic masks, attribute labels, and descriptive text, making it an ideal source for training advanced deep learning models. The dataset’s high-resolution quality, rich annotation information, and diverse representation contribute to the creation of realistic forgeries and enhance the effectiveness of forgery detection models.

3.2. Generation Method

Building on the high-quality foundation provided by the Multi-Modal-CelebA-HQ dataset, we have utilized a suite of 11 diffusion models to generate a diverse set of facial forgeries, as demonstrated in Fig. 2. The forgeries are devised through two principal methodologies: Unconditional Image Generation and Conditional Image Generation. For Unconditional Image Generation, we employ state-of-the-art diffusion models such as DDPM [14], DDIM [36], PNDM [22], P2 [8], and LDM [32]. These models synthesize facial images from pure noise, creating forgeries without reliance on any external data. In contrast, Conditional Image Generation is driven by additional, specific information that steers the generation process, including text prompts (Text-guided image generation), existing real images (Image-guided image generation), context cues (Inpaint), and manipulating identity and expression parameters (DiffSwap). We engage advanced models like Stable Diffusion 1.5, Stable Diffusion 2.1, and DiffSwap to produce highly detailed forgeries. Fig. 1 provides illustrative examples of our authentic images and the 11 types of forgeries generated, with additional displays set to be included in the supplementary materials. The details of each generation process are as follows:

Unconditional Image Generation In unconditional image generation, as depicted in Fig. 2 (a), our approach harnesses a spectrum of diffusion models to create synthetic images without the constraints of external data. Specifically, we employed a range of models: DDPM [14], inspired by non-equilibrium thermodynamics, excels at producing high-quality synthetic images. An alternative ap-

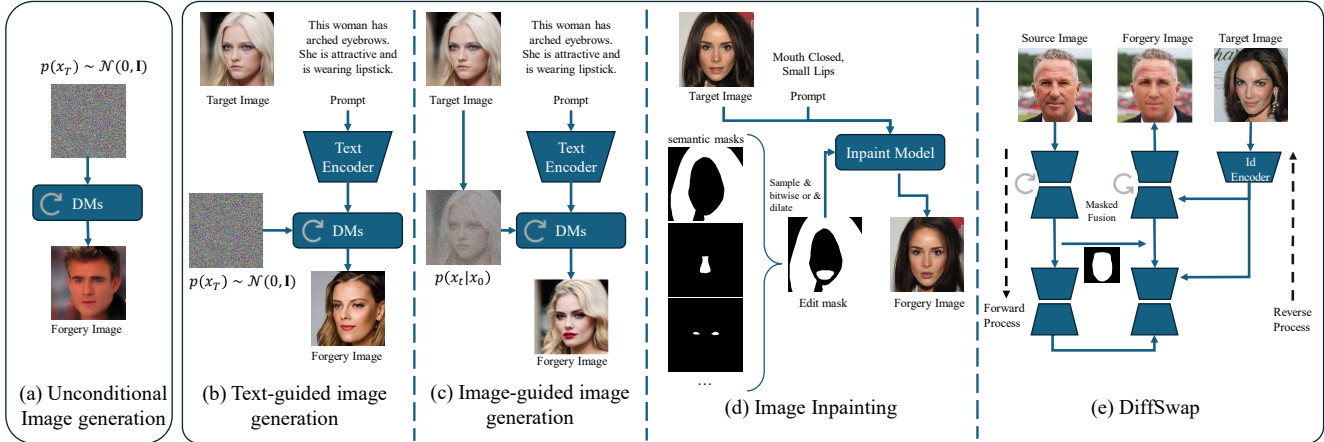


Figure 2. Pipeline of our face forgery approaches. (a) adopt pretrained diffusion models to generate forgery image directly. (b)-(e) represent conditional image generations conditioned on text prompts, image constraints, context cues, and identity, respectively.

proach is DDIM [36], which streamlines the sampling process, requiring fewer steps to achieve the desired results. PNDM [22], building upon DDPMs, views them as solvers of differential equations, enabling the generation of superior synthetic images in a mere 50 steps. P2 [8] stands as a lightweight version of the ADM [10] model but incorporates modified weight schemes, enhancing performance by allocating higher weights to perceptually rich content during diffusion steps. LDM [32], on the other hand, transforms images from pixel space to a more suitable latent space using adversarially trained autoencoders, which reduces computational complexity, enabling training at higher resolutions. Each of these diffusion models was employed with their pre-trained models on the CelebA dataset to generate 30,000 images in an unconditional manner.

Conditional Image Generation Building upon the foundation of Unconditional Image Generation, Conditional Image Generation introduces specificity to the forgery process. The generation of such images is informed by additional data, enabling the creation of forgeries that are not only realistic but also contextually coherent with the input conditions. This approach is essential for simulating more sophisticated forgery scenarios where specific attributes or characteristics are altered or preserved. The conditional methods span various techniques, each designed to manipulate or maintain certain aspects of the source data to produce the intended forgeries. We explore four distinct conditional generation methods: Text-guided image generation, Image-guided image generation, Image Inpainting, and Diffusion-based face swap. These methods allow us to customize the forgeries to exhibit particular traits or conform to certain scenarios, expanding the applicability of our dataset. We detail them as follows:

Text-guided image generation (Text2Img). To capture the nuanced relationship between descriptive language and facial features, we utilize text prompts as an additional condition. As depicted in Fig. 2 (b), we utilized Stable Diffusion versions 2.1 and 1.5 and selected three different textual prompts, randomly chosen from the MM-CelebA-HQ dataset, as conditions for generating face forgery images. These prompts were generated using attribute-based Probabilistic Context-Free Grammar (PCFG) and typically took the form of descriptions such as “A portrait image of a human face. He has big lips, a pointy nose, and straight hair”. This approach ensures a diverse range of facial characteristics are captured in our forgeries.

Image-guided image generation (Img2Img). Unlike general image generation detection, face forgery detection also involves assessing whether facial attributes have been tampered with. Since the manipulated images are based on original real images, detecting them is more challenging compared to generating entire images from scratch. As depicted in Fig. 2 (c), Img2Img is a method for generating modified counterfeit images based on input images and textual prompts. It utilizes a diffusion denoising mechanism proposed by SDEdit [26] to ensure that the output image retains the color and composition of the input image. The balance between the authenticity of the generated image and the fidelity of user input is controlled by adjusting the level of noise added during the forward SDE process. When creating the Img2Img dataset, we employed stable diffusion v1.5 and v2.1 checkpoints, and chose three commonly used t_0 parameters: 0.3, 0.5, and 0.7. Similar to Txt2Img, we employed corresponding image captions from MMCelebAHQ as prompts, gradually increasing the degree of image modification, as shown in Fig. 4a.

Image Inpainting (DiffInpaint). Image Inpainting is another technique for altering facial attributes, allowing for

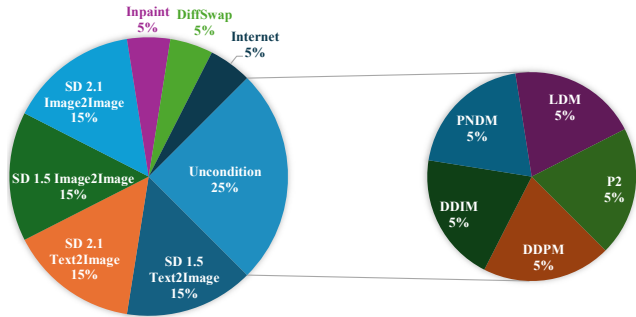


Figure 3. Illustration of the composition of the DiffusionFace dataset. Our dataset comprises 600,000 images, with 5% consisting of 30,000 images.

targeted alterations to specific image regions while leaving the rest of the image intact. As depicted in Fig. 2 (c), we initiate the process by sampling several semantic masks, combining them through bitwise-OR, and applying the dilate operation to obtain the final edit mask. Depending on the selected area, we generate a random attribute for it, serving as the text prompt. Fig. 4b demonstrates the utilization of attribute labels and semantic masks from MMCelebAHQ to modify facial images. During generation, we selected regions such as the nose, eyes, mouth, eyebrows, hair, and the entire face for modification. Each image had varying probabilities (0.25, 0.5, 0.25) of altering attributes in 1 to 3 regions. Sample attribute prompts for target modifications include phrases like “Narrow Eyes, Straight Eyebrows, Pointy Nos”, where the attribute is randomly selected.

Diffusion-based face swap (DiffSwap). DiffSwap [45] constitutes a diffusion model framework designed for high-fidelity and controllable facial swapping. Differing from other methods, DiffSwap possesses the capability to replace the original face with a chosen target face without altering the target character’s identity. Specifically, DiffSwap reconceptualizes face swapping as a conditional inpainting task guided by identity features and facial landmarks, with explicit shape consistency between the source and swapped faces. We employed the MM-CelebA-HQ dataset, randomly partitioning it into source and target faces and subsequently conducting random face swaps, ultimately generating 30,000 swapped images. The example is shown in Fig. 4c.

Furthermore, to assess the detection efficacy of DeepFake models on images sourced from the internet, we curated a dataset comprising images containing forgery faces, serving as an evaluation dataset representing real-world scenarios, with these images obtained from the website.

3.3. Dataset Detail

To ensure the integrity of image alignment and centering, particularly with text-guided Stable Diffusion and internet-

sourced images, we applied a standardization process. Using the facial detection capabilities of dlib [16], we filtered out excessively small facial regions and performed affine transformations for consistent alignment across our dataset. In instances where facial data quality was below our standards, we utilized the SSD-FIQA [28] for an unsupervised quality assessment, removing images that did not meet our benchmark. All images were resized to a uniform resolution of 256x256 pixels for consistency.

Statistically speaking, our DiffusionFace dataset comprises 30,000 genuine facial images from the high-fidelity MM-CelebA-HQ and an equal number of synthetic counterparts, generated using a diverse array of 11 diffusion techniques. Overall, the dataset includes 600,000 images, following the CelebA-HQ partitioning protocol with 480,000 images designated for training and 120,000 set aside for testing. As depicted in Fig. 3, the synthetic images were produced through a mix of internet-sourced forgery face images and 5 unconditional plus 6 conditional generation methods. Each method contributes 30,000 images, except for Text2Img and Img2Img, which employ three diverse prompts or parameters, yielding a total of 90,000 images. This blend ensures a rich variety in our dataset, further augmented by the inclusion of internet-sourced images to reflect the diversity encountered in real-world applications.

4. Experiments

4.1. Frequency Analysis

The images generated by diffusion models have reached a quality level where they are virtually indistinguishable from real images. However, in the detection of GAN images, certain artifacts in the frequency domain become evident, distinguishing them from natural images. In this section, we analyze the distinctions between images generated by diffusion models and real images in the frequency domain. We employ a common frequency domain transformation method: Discrete Fourier Transform (DFT).

Fig. 5 depicts the average absolute DFT spectrum of 3k images from each diffusion method in our dataset, the pre-process following prior research [39]. Facial images, in contrast to natural images, present a more distinct spectral shape owing to the homogeneity of the dataset. Observations reveal that images generated using Img2Img, Inpaint, DiffSwap, and LDM methods display noticeable artifacts in the frequency domain. Conversely, P2 and Stable Diffusion T2I exhibit frequency domain images most similar to real images, while DDPM, DDIM, and PNDM-generated images exhibit deviations from real images in the high-frequency region.

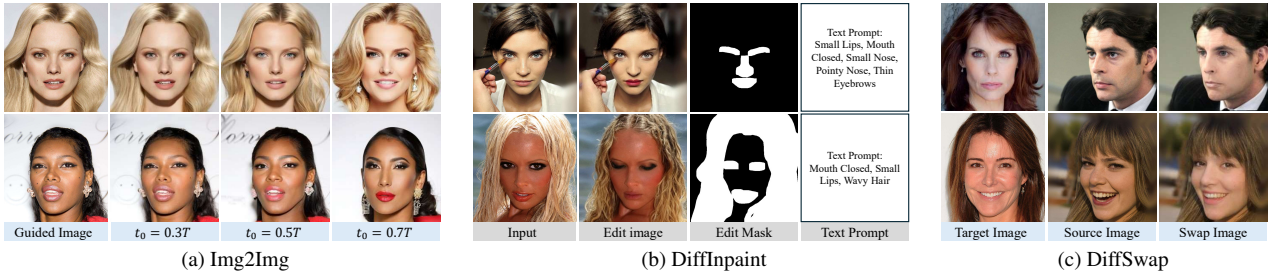


Figure 4. Visualization of Image-Guided Image Generation, Image Inpainting and Diffusion-Based Face Swap. In Img2Img, images are generated with varying t_0 parameters, progressively increasing the modification. In DiffInpaint, the diffusion model modifies only the masked area based on the image context. In DiffSwap, only the identity is altered.

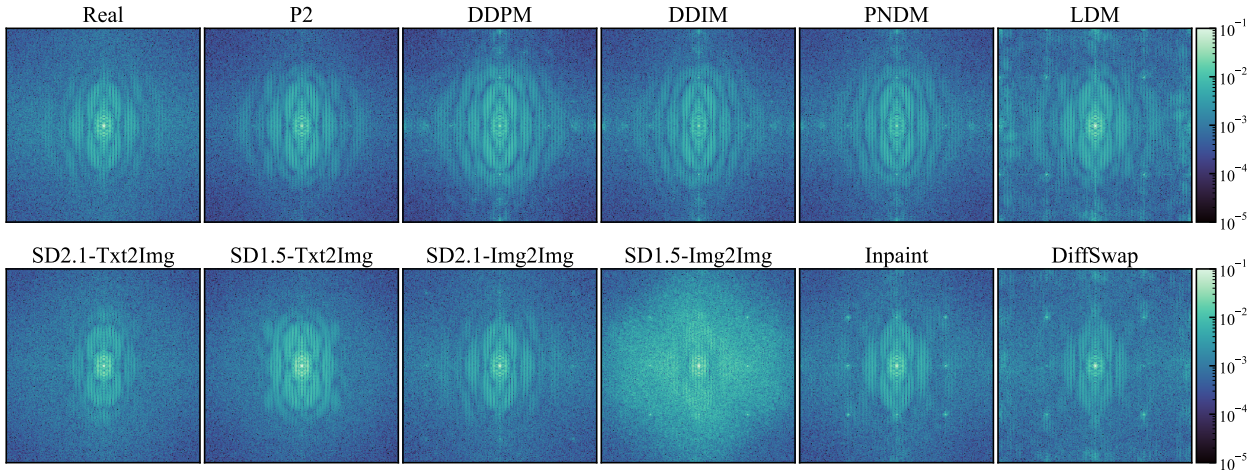


Figure 5. Mean of the DFT spectrum from real and generated images.

4.2. Fake Image Detections

In this section, we initiate the evaluation by assessing the performance of state-of-the-art fake image detectors and face forgery detectors on DM-generated images. To measure the effectiveness of these detection methods in real-world scenarios, we employ five distinct evaluation settings. Within-domain and cross-model testing entail the use of images generated by diffusion models that are either identical or distinct from those in the training dataset. In post-processing testing, we simulate the effects of compression or resampling operations that images may undergo during internet upload and download. Cross-data testing employs different datasets for generating training and testing images, with models that can be the same or different. “In the wild” testing involves detecting fake images found circulating on the internet. A detailed breakdown of these settings follows in the subsequent subsections.

Within-domain and cross-domain testing Within-domain testing is the simplest scenario, while cross-model

testing emulates real-world situations where the identity of the face forgery image generator is unknown and potentially evolving. In our study, we initiate the evaluation by assessing the performance of a conventional CNN-generated image detector, CNNDetection [39], and present detailed metrics. For other models, including CR [7], F3Net [30], GramNet [24], MAT [44], GFF [25], DCL [38], UniDetection [27], RECCE [6] and SAIA [37], we provide the average scores achieved when training on various subsets and testing on specific subsets.

The detailed results of CNNDetection are depicted in Fig. 2. In the context of Unconditional Image Generation, the detector trained with P2 exhibits robust generalization capabilities, extending well to other Unconditional Image Generation methods. However, it struggles when applied to images generated through Conditional Image Generation. Among counterfeit images generated by Stable Diffusion, detectors trained on Stable Diffusion v2.1 Img2Img achieve the best generalization, while those trained using Text2Img exhibit a significant drop in performance when detecting Img2Img images. Detectors trained with the Inpainting

Train on	Unconditional Image Generation (Test Dataset)					Conditional Image Generation (Test Dataset)						Average Auc(%)
	DDPM	DDIM	PNDM	P2	LDM	SDv1.5 I2I	SDv1.5 T2I	SDv2.1 I2I	SDv2.1 T2I	Inpaint	DiffSwap	
DDPM	99.9	99.9	99.9	82.8	54.5	37.7	23.2	61.1	29.2	54.5	63.1	63.4
DDIM	100.0	100.0	100.0	82.6	52.1	42.6	41.3	58.6	41.4	52.4	72.3	67.6
PNDM	100.0	100.0	100.0	80.2	38.4	39.5	30.6	58.5	34.8	54.4	70.3	64.2
P2	99.6	96.9	98.0	100.0	96.4	86.7	72.6	87.8	55.3	63.5	77.1	84.9
LDM	90.1	78.5	81.5	89.2	100.0	87.9	66.1	88.1	38.8	70.8	77.2	78.9
SDv1.5 I2I	68.6	74.3	74.8	58.1	66.9	100.0	98.0	79.8	86.7	86.4	48.3	76.5
SDv1.5 T2I	50.6	62.7	64.1	51.6	67.5	96.2	100.0	77.7	100.0	84.9	58.3	74.0
SDv2.1 I2I	81.6	85.4	85.4	70.9	80.6	99.6	95.9	100.0	97.7	86.4	58.5	85.6
SDv2.1 T2I	46.3	55.6	56.8	46.1	51.3	82.7	100.0	81.9	100.0	59.6	45.4	66.0
Inpaint	92.2	93.9	92.4	53.9	80.4	100.0	99.7	92.6	73.2	100.0	61.0	85.4
DiffSwap	74.2	74.1	73.6	62.2	82.0	51.2	48.0	63.6	31.1	61.2	100.0	65.6

Table 2. Result of with-domain and cross-domain on different training and testing subsets using CNNDetection.

Models	Unconditional Image Generation										Conditional Image Generation										Average			
	DDPM		DDIM		PNDM		P2		LDM		SDv1.5 I2I		SDv1.5 T2I		SDv2.1 I2I		SDv2.1 T2I		Inpaint				DiffSwap	
	ACC	AUC	ACC	AUC	ACC	AUC	ACC	AUC	ACC	AUC	ACC	AUC	ACC	AUC	ACC	AUC	ACC	AUC	ACC	AUC	ACC	AUC	ACC	AUC
CNNDetection	67.2	82.1	67.1	83.8	67.5	84.2	54.9	70.7	57.5	70.0	65.1	74.9	67.7	70.5	55.9	77.2	62.8	62.6	56.5	70.4	54.7	67.1	61.5	74.0
CR	67.6	82.4	67.2	83.9	67.7	84.3	55.3	73.0	58.3	71.0	65.1	75.4	67.1	68.2	55.7	73.4	63.0	61.6	56.4	68.9	54.8	68.0	61.7	73.7
F3Net	67.7	62.8	60.9	80.3	61.1	79.9	54.5	67.8	61.6	72.6	62.0	71.0	63.9	68.2	54.7	67.7	61.0	62.5	56.1	67.6	54.6	65.6	59.8	69.6
GramNet	69.8	72.2	69.9	79.2	70.0	79.2	54.6	67.4	59.5	77.2	64.6	74.2	68.3	73.7	55.6	76.1	62.5	62.6	59.0	68.9	54.7	66.7	62.6	72.5
MAT	66.9	81.5	67.1	83.6	67.5	84.0	54.6	66.8	57.8	69.1	65.0	74.3	67.4	68.3	56.4	78.3	62.1	59.0	56.8	72.3	54.8	68.9	61.5	73.3
GFF	66.8	83.8	67.0	86.0	67.5	86.2	54.6	62.6	58.0	61.1	64.6	74.5	66.2	67.5	55.2	76.3	61.2	58.6	56.7	72.8	54.7	67.8	61.1	72.5
DCL	67.2	77.2	67.3	78.1	67.9	78.9	55.9	69.7	60.0	72.8	65.0	73.4	68.8	71.9	57.4	73.6	63.1	63.4	57.1	68.5	55.4	67.2	62.3	72.3
UniDetection	65.0	72.5	73.3	76.1	72.5	76.6	61.5	81.5	66.9	79.5	57.6	60.7	65.0	79.5	52.7	59.2	61.1	76.6	54.6	53.7	58.9	74.5	62.7	71.8
RECCE	76.5	74.6	72.7	80.1	72.5	80.5	54.8	66.1	66.9	74.5	63.2	65.9	68.1	69.7	55.1	70.9	61.6	69.6	62.0	66.9	54.6	65.3	64.4	71.3
SAIA	67.1	80.2	67.2	82.1	67.8	82.8	55.7	72.2	59.1	75.8	65.1	73.6	68.2	72.7	56.5	77.9	62.5	65.3	56.8	70.4	54.9	68.6	61.9	74.7

Table 3. Within-domain and cross-domain detection average performance on different models.

method excel at identifying counterfeit images generated by Stable Diffusion v1.5, but the reverse is not true.

Tab. 3 displays the average performance of different methods. Each row in the table represents the vertical average of the metrics shown in Tab. 2, signifying the average performance when trained on different subsets and tested on specified datasets. The results indicate that UniDetection generalizes well in unconditional image generation but struggles with certain conditional image generation methods. Among these methods, RECCE and SAIA exhibit the best performance in terms of ACC and AUC. However, none of the methods for GAN-based image detection or face forgery detection demonstrate a high level of generality in diffusion-based face forgery detection.

post-processing testing Images uploaded and downloaded from the internet often undergo various post-processing steps, such as compression and resampling. On the other hand, images may be manipulated to reduce their detectability, for instance, through blurring and noise addition. In post-processing testing, we used the SD v2.1 Img2Img dataset for training, which demonstrated the best overall performance in both within-domain and cross-domain testing. It is important to note that the models

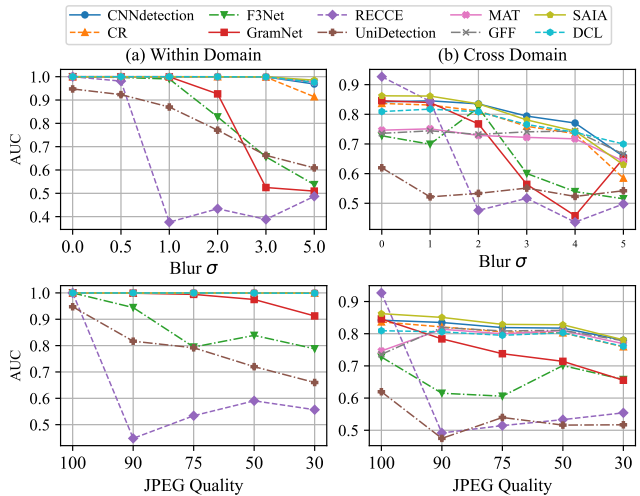


Figure 6. Within-domain and cross-domain model performance training on different model in various Blur σ and Jpeg Quality.

tested in the following sections were trained on the SD v2.1 Img2Img dataset by default, unless otherwise specified. We reported the within-domain and average cross-domain AUC metrics under various conditions, evaluating the model's

Test-Dataset	Forgery Generator	CNNDetection		CR		F3Net		GramNet		MAT		GFF		DCL		UniDetection		RECCE		SAIA		degradation	
		ACC	EER	ACC	EER	ACC	EER	ACC	EER	ACC	EER	ACC	EER	ACC	EER	ACC	EER	ACC	EER	ACC	EER	ACC	EER
CelebA-HQ FFHQ	LDM	99.9	0.10	99.9	0.06	100.0	0.00	99.9	0.01	99.9	0.03	99.9	0.01	99.6	0.31	97.7	0.88	100.0	0.00	99.9	0.05	-	-
	LDM	87.8	2.36	90.4	1.63	49.9	60.6	49.6	84.0	91.3	1.63	87.8	2.10	88.0	5.48	49.0	43.83	49.9	51.11	91.9	2.86	-26.11	+25.41
CelebA-HQ FFHQ	P2	99.9	0.06	99.8	0.14	99.9	0.00	99.9	0.06	99.8	0.11	99.8	0.11	99.4	0.54	98.4	1.55	100.0	0.00	99.7	0.24	-	-
	P2	93.5	4.46	92.8	5.36	87.6	10.28	93.2	6.74	91.6	1.63	94.5	5.44	89.1	5.93	68.8	16.01	74.0	31.98	92.2	4.26	-11.9	+8.92

Table 4. Cross-data model performance training on CelebA-HQ and tests on CelebA-HQ and FFHQ. The diffusion generators are LDM and P2.

Methods	Forgery Generator				
	SDv2.1 T2I	SDv2.1 I2I	Inpaint	P2	LDM
CNNDetection	54.3 / 80.7	93.6 / 98.9	65.1 / 92.0	50.9 / 47.4	51.9 / 64.5
CR	56.5 / 87.4	93.6 / 98.5	67.5 / 91.8	50.7 / 40.5	53.4 / 65.6
F3Net	61.9 / 90.6	80.6 / 95.6	50.3 / 44.0	51.6 / 54.6	50.2 / 37.3
GramNet	57.3 / 87.1	91.2 / 98.1	72.8 / 87.9	51.1 / 51.5	51.4 / 63.3
MAT	54.3 / 77.3	87.6 / 96.6	63.2 / 88.3	50.6 / 44.5	52.3 / 74.3
GFF	54.2 / 83.4	89.9 / 97.5	63.1 / 88.1	51.0 / 53.3	52.3 / 65.4
DCL	55.8 / 79.7	90.3 / 97.2	66.5 / 87.6	50.8 / 50.1	53.1 / 66.2
UniDetection	62.6 / 71.2	50.0 / 73.4	68.3 / 74.4	55.1 / 57.4	56.3 / 66.2
RECCE	57.6 / 95.2	91.7 / 98.6	50.9 / 80.0	60.8 / 94.7	50.3 / 60.4
SAIA	54.7 / 84.2	89.7 / 98.0	66.2 / 93.1	50.8 / 44.5	52.9 / 72.6
Average	<u>57.7 / 83.0</u>	87.9 / 95.5	63.5 / 80.3	53.3 / 56.7	53.0 / 65.8

Table 5. In the wild testing model performance. We report ACC / AUC(%) in the table.

sensitivity to blur and JPEG compression, as depicted in Fig. 6.

In the absence of Jpeg compression or blur, RECCE, utilizing reconstruction-classification learning, initially demonstrated superior performance, but it faced challenges in scenarios involving post-processing. Conversely, SAIA consistently exhibited strong performance and demonstrated resilience to post-processing effects. UniDetection, relying on a frozen pretrained CLIP as a backbone with minimal parameter fine-tuning, struggled to adapt to the challenging Img2Img dataset, resulting in inferior performance. Notably, all models experienced a more pronounced performance drop when detecting compressed images compared to within-domain testing. This implies that there is room for enhancing the performance of these models in detecting compressed images within a cross-domain context.

Cross-data testing In the real world, different datasets are employed to train generative models, each with its own unique biases and preprocessing methods that can significantly impact the generated images. Hence, it’s essential to assess the model’s ability to generalize to unfamiliar images used in training generative models. In such a setup, the data used to generate training images differs from the data used to generate test images.

In our study, we evaluated the performance of models trained on CelebA-HQ images in detecting FFHQ test images. Real images are sourced from the FFHQ dataset,

while fake images are generated by diffusion models trained on FFHQ data. The results presented in Tab. 4 highlight a performance degradation when detectors trained on CelebA-HQ data are transferred to FFHQ data. Notably, RECCE, UniDetection, F3Net, and GramNet exhibit a noticeable decline, especially when trained on LDM-generated images. This decline is attributed to these models overfitting to prominent artifacts in the LDM-generated images, resulting in reduced generalization. In contrast, P2-generated images lack such artifacts, rendering their learned features more transferable. Other methods, such as MAT and SAIA, demonstrate more robust performance, experiencing minimal degradation when tested on the FFHQ dataset.

In the wild This scenario simulates a real-world situation in which detection models may encounter authentic images generated by different generative models, diverse generation methods, or various post-processing techniques and hyperparameters. In such cases, detection models must adapt to emerging new-generation technologies, presenting a challenging real-world scenario. To simulate this context, we additionally collected 30,000 genuine facial images sourced from online media. These images were generated by unknown models, primarily from the Stable Diffusion family, and featured a variety of additional settings, including LoRA, different sampling methods, and super-resolution, among others.

As illustrated in Tab. 5, we have selected several representative data displays, which, as expected, demonstrate strong generality in models trained on CNNDetection (Tab. 2). As expected, detectors trained on data generated using Stable Diffusion exhibit higher performance. It is worth noting that detectors trained on data generated using Img2Img show better results than Txt2Img. This could be attributed to the fact that the counterfeit data generated by Img2Img is more similar to the original data, prompting the model to uncover more generalized forgery features.

5. Conclusion

This paper introduces the first diffusion-based facial forgery dataset, encompassing various forgery categories. Our dataset and evaluation protocol provide a foundational basis for enhancing the security of facial image

authentication processes. Furthermore, our study assesses the effectiveness of various image detection methods in real-world scenarios, employing five different evaluation settings for detailed analysis. Performance variations exist among different image detection methods in real-world scenarios, and detection models must continually adapt to new technologies to combat the evolving landscape of counterfeit images generated by different models and techniques.

References

- [1] Faceswap. <https://github.com/MarekKowalski/FaceSwap/>. 1
- [2] Fakeapp. <https://www.fakeapp.com/>, 2018. 1
- [3] faceswap-gan. <https://github.com/shaoanlu/faceswap-GAN>, 2019. 1
- [4] Roberto Amoroso, Davide Morelli, Marcella Cornia, Lorenzo Baraldi, Alberto Del Bimbo, and Rita Cucchiara. Parents and children: Distinguishing multimodal deepfakes from natural images. *arXiv preprint arXiv:2304.00500*, 2023. 2, 3
- [5] Jordan J Bird and Ahmad Lotfi. Cifake: Image classification and explainable identification of ai-generated synthetic images. *arXiv preprint arXiv:2303.14126*, 2023. 1, 2, 3
- [6] Junyi Cao, Chao Ma, Taiping Yao, Shen Chen, Shouhong Ding, and Xiaokang Yang. End-to-end reconstruction-classification learning for face forgery detection. In *Proceedings of the IEEE/CVF Conference on Computer Vision and Pattern Recognition*, pages 4113–4122, 2022. 6, 1
- [7] Keshigeyan Chandrasegaran, Ngoc-Trung Tran, Alexander Binder, and Ngai-Man Cheung. Discovering transferable forensic features for cnn-generated images detection. In *European Conference on Computer Vision*, pages 671–689. Springer, 2022. 6, 1
- [8] Jooyoung Choi, Jungbeom Lee, Chaehun Shin, Sungwon Kim, Hyunwoo Kim, and Sungroh Yoon. Perception prioritized training of diffusion models. In *Proceedings of the IEEE/CVF Conference on Computer Vision and Pattern Recognition*, pages 11472–11481, 2022. 2, 3, 4
- [9] Hao Dang, Feng Liu, Joel Stehouwer, Xiaoming Liu, and Anil K Jain. On the detection of digital face manipulation. In *CVPR*, pages 5781–5790, 2020. 2
- [10] Prafulla Dhariwal and Alexander Nichol. Diffusion models beat gans on image synthesis. *Advances in neural information processing systems*, 34:8780–8794, 2021. 4
- [11] Brian Dolhansky, Russ Howes, Ben Pflaum, Nicole Baram, and Cristian Canton Ferrer. The deepfake detection challenge (dfdc) preview dataset. *arXiv preprint arXiv:1910.08854*, 2019. 3
- [12] Ian Goodfellow, Jean Pouget-Abadie, Mehdi Mirza, Bing Xu, David Warde-Farley, Sherjil Ozair, Aaron Courville, and Yoshua Bengio. Generative adversarial nets. *Advances in neural information processing systems*, 27, 2014. 1
- [13] Yanan He, Bei Gan, Siyu Chen, Yichun Zhou, Guojun Yin, Luchuan Song, Lu Sheng, Jing Shao, and Ziwei Liu. Forgerynet: A versatile benchmark for comprehensive forgery analysis. In *Proceedings of the IEEE/CVF conference on computer vision and pattern recognition*, pages 4360–4369, 2021. 1, 2, 3
- [14] Jonathan Ho, Ajay Jain, and Pieter Abbeel. Denoising diffusion probabilistic models. *Advances in neural information processing systems*, 33:6840–6851, 2020. 1, 2, 3
- [15] Liming Jiang, Ren Li, Wayne Wu, Chen Qian, and Chen Change Loy. Deepforensics-1.0: A large-scale dataset for real-world face forgery detection. In *CVPR*, 2020. 3
- [16] Davis E King. Dlib-ml: A machine learning toolkit. *The Journal of Machine Learning Research*, 10:1755–1758, 2009. 5
- [17] Diederik P Kingma and Max Welling. Auto-encoding variational bayes. *arXiv preprint arXiv:1312.6114*, 2013. 1
- [18] Pavel Korshunov and Sébastien Marcel. Deepfakes: a new threat to face recognition? assessment and detection. *arXiv preprint arXiv:1812.08685*, 2018. 3
- [19] Alex Krizhevsky and Geoff Hinton. Convolutional deep belief networks on cifar-10. *Unpublished manuscript*, 40(7): 1–9, 2010. 3
- [20] Yuezun Li, Xin Yang, Pu Sun, Honggang Qi, and Siwei Lyu. Celeb-df: A large-scale challenging dataset for deepfake forensics. In *Proceedings of the IEEE/CVF conference on computer vision and pattern recognition*, pages 3207–3216, 2020. 1, 2, 3
- [21] Tsung-Yi Lin, Michael Maire, Serge Belongie, James Hays, Pietro Perona, Deva Ramanan, Piotr Dollár, and C Lawrence Zitnick. Microsoft coco: Common objects in context. In *Computer Vision—ECCV 2014: 13th European Conference, Zurich, Switzerland, September 6–12, 2014, Proceedings, Part V 13*, pages 740–755. Springer, 2014. 3
- [22] Luping Liu, Yi Ren, Zhijie Lin, and Zhou Zhao. Pseudo numerical methods for diffusion models on manifolds. In *International Conference on Learning Representations*, 2022. 2, 3, 4
- [23] Ziwei Liu, Ping Luo, Xiaogang Wang, and Xiaoou Tang. Deep learning face attributes in the wild. In *Proceedings of International Conference on Computer Vision (ICCV)*, 2015. 3
- [24] Zhengzhe Liu, Xiaojuan Qi, and Philip HS Torr. Global texture enhancement for fake face detection in the wild. In *CVPR*, 2020. 6, 1
- [25] Yuchen Luo, Yong Zhang, Junchi Yan, and Wei Liu. Generalizing face forgery detection with high-frequency features. In *Proceedings of the IEEE/CVF conference on computer vision and pattern recognition*, pages 16317–16326, 2021. 6, 1
- [26] Chenlin Meng, Yutong He, Yang Song, Jiaming Song, Jiajun Wu, Jun-Yan Zhu, and Stefano Ermon. Sdedit: Guided image synthesis and editing with stochastic differential equations. *arXiv preprint arXiv:2108.01073*, 2021. 4
- [27] Utkarsh Ojha, Yuheng Li, and Yong Jae Lee. Towards universal fake image detectors that generalize across generative models. In *Proceedings of the IEEE/CVF Conference on Computer Vision and Pattern Recognition*, pages 24480–24489, 2023. 6, 1

- [28] Fu-Zhao Ou, Xingyu Chen, Ruixin Zhang, Yuge Huang, Shaoxin Li, Jilin Li, Yong Li, Liujuan Cao, and Yuan-Gen Wang. Sdd-fiq: unsupervised face image quality assessment with similarity distribution distance. In *Proceedings of the IEEE/CVF conference on computer vision and pattern recognition*, pages 7670–7679, 2021. 5
- [29] Ivan Petrov, Daiheng Gao, Nikolay Chervoniy, Kunlin Liu, Sugasa Marangonda, Chris Umé, Jian Jiang, Luis RP, Sheng Zhang, Pingyu Wu, et al. Deepfacelab: A simple, flexible and extensible face swapping framework. *arXiv preprint arXiv:2005.05535*, 2020. 1
- [30] Yuyang Qian, Guojun Yin, Lu Sheng, Zixuan Chen, and Jing Shao. Thinking in frequency: Face forgery detection by mining frequency-aware clues. In *ECCV*, 2020. 6, 1
- [31] Jonas Ricker, Simon Damm, Thorsten Holz, and Asja Fischer. Towards the detection of diffusion model deepfakes. *arXiv preprint arXiv:2210.14571*, 2022. 1, 2, 3
- [32] Robin Rombach, Andreas Blattmann, Dominik Lorenz, Patrick Esser, and Björn Ommer. High-resolution image synthesis with latent diffusion models. In *Proceedings of the IEEE/CVF Conference on Computer Vision and Pattern Recognition (CVPR)*, pages 10684–10695, 2022. 1, 2, 3, 4
- [33] Andreas Rossler, Davide Cozzolino, Luisa Verdoliva, Christian Riess, Justus Thies, and Matthias Nießner. Faceforensics++: Learning to detect manipulated facial images. In *Proceedings of the IEEE/CVF international conference on computer vision*, pages 1–11, 2019. 1, 2, 3
- [34] Zeyang Sha, Zheng Li, Ning Yu, and Yang Zhang. Defake: Detection and attribution of fake images generated by text-to-image diffusion models. *arXiv preprint arXiv:2210.06998*, 2022. 1, 2, 3
- [35] Jascha Sohl-Dickstein, Eric Weiss, Niru Maheswaranathan, and Surya Ganguli. Deep unsupervised learning using nonequilibrium thermodynamics. In *International conference on machine learning*, pages 2256–2265. PMLR, 2015. 1
- [36] Jiaming Song, Chenlin Meng, and Stefano Ermon. Denoising diffusion implicit models. *arXiv preprint arXiv:2010.02502*, 2020. 2, 3, 4
- [37] Ke Sun, Hong Liu, Taiping Yao, Xiaoshuai Sun, Shen Chen, Shouhong Ding, and Rongrong Ji. An information theoretic approach for attention-driven face forgery detection. In *European Conference on Computer Vision*, pages 111–127. Springer, 2022. 6, 1
- [38] Ke Sun, Taiping Yao, Shen Chen, Shouhong Ding, Jilin Li, and Rongrong Ji. Dual contrastive learning for general face forgery detection. In *Proceedings of the AAAI Conference on Artificial Intelligence*, pages 2316–2324, 2022. 6, 1
- [39] Sheng-Yu Wang, Oliver Wang, Richard Zhang, Andrew Owens, and Alexei A Efros. Cnn-generated images are surprisingly easy to spot... for now. In *Proceedings of the IEEE/CVF conference on computer vision and pattern recognition*, pages 8695–8704, 2020. 5, 6, 1
- [40] Zhendong Wang, Jianmin Bao, Wengang Zhou, Weilun Wang, Hezhen Hu, Hong Chen, and Houqiang Li. Dire for diffusion-generated image detection. *arXiv preprint arXiv:2303.09295*, 2023. 2, 3
- [41] Weihao Xia, Yujiu Yang, Jing-Hao Xue, and Baoyuan Wu. Tedigan: Text-guided diverse face image generation and manipulation. In *IEEE Conference on Computer Vision and Pattern Recognition (CVPR)*, 2021. 2, 3
- [42] Xin Yang, Yuezun Li, and Siwei Lyu. Exposing deep fakes using inconsistent head poses. In *ICASSP*, 2019. 2, 3
- [43] Fisher Yu, Ari Seff, Yinda Zhang, Shuran Song, Thomas Funkhouser, and Jianxiong Xiao. Lsun: Construction of a large-scale image dataset using deep learning with humans in the loop. *arXiv preprint arXiv:1506.03365*, 2015. 3
- [44] Hanqing Zhao, Wenbo Zhou, Dongdong Chen, Tianyi Wei, Weiming Zhang, and Nenghai Yu. Multi-attentional deepfake detection. In *Proceedings of the IEEE/CVF conference on computer vision and pattern recognition*, pages 2185–2194, 2021. 6, 1
- [45] Wenliang Zhao, Yongming Rao, Weikang Shi, Zuyan Liu, Jie Zhou, and Jiwen Lu. Diffswap: High-fidelity and controllable face swapping via 3d-aware masked diffusion. *CVPR*, 2023. 2, 5
- [46] Mingjian Zhu, Hanting Chen, Qiangyu Yan, Xudong Huang, Guanyu Lin, Wei Li, Zhijun Tu, Hailin Hu, Jie Hu, and Yunhe Wang. Genimage: A million-scale benchmark for detecting ai-generated image. *arXiv preprint arXiv:2306.08571*, 2023. 1, 2, 3
- [47] Bojia Zi, Minghao Chang, Jingjing Chen, Xingjun Ma, and Yu-Gang Jiang. Wilddeepfake: A challenging real-world dataset for deepfake detection. In *Proceedings of the 28th ACM international conference on multimedia*, pages 2382–2390, 2020. 2

DiffusionFace: Towards a Comprehensive Dataset for Diffusion-Based Face Forgery Analysis

Supplementary Material

Due to the page limit of the paper, we provide a more comprehensive description and experimental results in this supplementary. The main content is organized into the following sections: 1) Elaboration on forgery detectors is provided in Section 6. 2) Further within-domain and cross-domain testing results are presented in Section 7. 3) Section 8 contains t-SNE feature visualizations trained for binary and multiclass classification. 4) Additional visualizations pertaining to the DiffusionFace dataset are available in Section 9.

6. More Detailed of Forgery Detectors

We employ a total of 10 forgery detectors at the image level, comprising three general generated image detectors (CNNDetection [39], CR [7], UniDetection [27]), and eight deepfake detectors (F3Net [30], GramNet [24], MAT [44], GFF [25], DCL [38], RECCE [6], and SAIA [37]).

- **CNNDetection:** A conventionally trained detector, CNNDetection uses ProGAN-generated images for training, implementing JPEG compression, blurring, and scaling for data augmentation. Its trained classifier boasts impressive generalization abilities across different datasets, network architectures, and training tasks.
- **Color-Robust (CR) Universal Detector:** This detector addresses generic detectors’ susceptibility to color-misleading forgeries by eliminating color dependence in cross-mode computer forensics. It achieves this by randomly removing color information from samples during training.
- **UniDetection:** By classifying authenticity within the feature space of the pre-trained CLIP model, UniDetection significantly improves the generalization of fake image detection.
- **F3Net:** This detector utilizes two distinct yet complementary frequency-sensitive indices to reveal forgery patterns, incorporating the Discrete Cosine Transform (DCT) as an applied frequency domain transformation, introducing frequency elements into facial forgery detection.
- **GramNet:** Noticing the distinct texture differences between fake and real human faces, GramNet leverages global image texture representation for robust fake image detection, as global texture statistics are more robust.
- **MAT:** By framing Deepfake detection as a fine-grained classification problem, MAT uses multiple spatial attention heads to focus on different local regions, texture feature enhancement blocks to amplify subtle artifacts in

shallow features, and aggregates low-level texture features and high-level semantic features guided by the attention map.

- **GFF:** Utilizing multi-scale high-frequency noises for face forgery detection, GFF introduces the residual-guided spatial attention module to guide the low-level RGB stream.
- **DCL:** This method constructs positive and negative paired data and performs contrastive learning at different granularities to learn generalized feature representation.
- **RECCE:** Emphasizing common compact representations of genuine faces based on reconstruction-classification learning, RECCE proposes a forgery detection framework.
- **SAIA:** Observing that forgery clues are often hidden in informative regions, SAIA introduces the self-information metric to enhance feature representation for forgery detection.

7. More Detailed Results of Trained on Different Detectors

We present detailed results from within-domain and cross-domain testing, utilizing F3Net, RECCE, UniDetection, and SAIA. Refer to Tables 6, 7, 8, and 9 for a comprehensive overview of the performance on various training and testing subsets.

As discussed in the main manuscript, nearly all detectors trained on Stable Diffusion v2.1 Img2Img demonstrate commendable generalization, with the exception of UniDetection. This discrepancy may stem from UniDetection’s utilization of a pre-trained CLIP model with fixed weights as a feature extractor, hindering its convergence during training on the Img2Img dataset.

8. Feature Space Visualization

In this section, we explore the visualization of feature spaces derived from binary and multiclass classification using t-SNE, a potent technique for representing high-dimensional data in a lower-dimensional space. To accomplish this, we employ CNNDetection as detector, utilizing the features extracted from the last fully connected layer to generate the t-SNE visualizations.

Binary classification We illustrate the t-SNE features obtained through binary classification on a mixed dataset, as

Train on	Unconditional Image Generation (Test Dataset)					Conditional Image Generation (Test Dataset)						Average Auc(%)
	DDPM	DDIM	PNDM	P2	LDM	SDv1.5 I2I	SDv1.5 T2I	SDv2.1 I2I	SDv2.1 T2I	Inpaint	DiffSwap	
DDPM	<u>100.0</u>	99.9	99.9	69.2	25.0	51.5	30.8	49.5	21.5	49.7	50.5	58.9
DDIM	100.0	<u>100.0</u>	100.0	89.6	43.4	60.8	52.9	54.0	32.1	56.7	80.7	70.0
PNDM	100.0	100.0	<u>100.0</u>	52.0	54.6	50.2	40.2	43.7	45.0	50.2	68.1	64.0
P2	74.9	93.4	93.7	<u>100.0</u>	97.1	66.4	64.0	74.5	58.8	63.7	57.0	76.7
LDM	36.1	70.8	69.5	93.2	<u>100.0</u>	56.2	43.1	57.6	62.5	63.4	81.3	66.7
SDv1.5 I2I	54.9	60.2	60.4	53.0	58.9	<u>100.0</u>	97.4	76.6	86.3	89.1	46.1	71.2
SDv1.5 T2I	27.7	75.4	74.9	56.5	94.4	94.3	<u>100.0</u>	79.4	99.9	84.5	75.7	78.4
SDv2.1 I2I	98.9	42.7	43.4	56.3	59.8	97.4	97.5	<u>99.9</u>	90.2	91.1	49.8	<u>75.2</u>
SDv2.1 T2I	18.5	67.1	67.8	67.3	96.6	64.7	99.9	77.5	<u>100.0</u>	55.8	74.6	71.8
Inpaint	49.9	94.4	91.2	49.3	68.3	99.9	72.5	86.2	35.6	<u>99.9</u>	37.0	71.3
DiffSwap	29.3	78.9	77.7	59.0	99.8	38.7	51.0	44.8	55.0	38.8	<u>100.0</u>	61.2

Table 6. Result of with-domain and cross-domain on different training and testing subsets using F3Net.

Train on	Unconditional Image Generation (Test Dataset)					Conditional Image Generation (Test Dataset)						Average Auc(%)
	DDPM	DDIM	PNDM	P2	LDM	SDv1.5 I2I	SDv1.5 T2I	SDv2.1 I2I	SDv2.1 T2I	Inpaint	DiffSwap	
DDPM	<u>100.0</u>	99.9	99.9	69.7	45.4	59.8	47.7	72.4	62.1	65.2	54.5	70.6
DDIM	100.0	<u>100.0</u>	100.0	56.8	38.9	52.1	54.5	66.8	66.7	56.9	52.1	67.7
PNDM	100.0	100.0	<u>100.0</u>	63.9	47.3	59.8	29.9	66.9	41.1	59.3	62.7	66.4
P2	73.3	78.1	79.0	<u>100.0</u>	97.9	37.8	92.0	91.8	80.5	35.3	67.2	75.7
LDM	32.9	24.1	28.2	72.3	<u>100.0</u>	38.9	66.2	56.9	67.4	43.4	63.7	54.0
SDv1.5 I2I	99.6	92.6	89.9	50.9	99.4	<u>100.0</u>	96.2	65.3	73.5	99.9	47.9	<u>83.2</u>
SDv1.5 T2I	22.4	73.0	72.9	69.3	90.4	77.0	<u>100.0</u>	66.1	99.9	71.1	77.1	74.5
SDv2.1 I2I	100.0	99.7	99.8	92.2	80.2	99.9	99.4	<u>100.0</u>	89.5	99.7	65.9	93.3
SDv2.1 T2I	40.7	53.2	55.6	53.0	81.8	52.4	99.9	60.9	<u>100.0</u>	52.4	72.9	65.7
Inpaint	100.0	99.0	99.2	49.2	38.1	100.0	56.0	87.0	50.1	<u>100.0</u>	54.4	75.7
DiffSwap	51.1	60.7	60.9	49.7	99.9	46.9	23.8	44.9	34.3	52.7	<u>100.0</u>	56.8

Table 7. Result of with-domain and cross-domain on different training and testing subsets using RECCE.

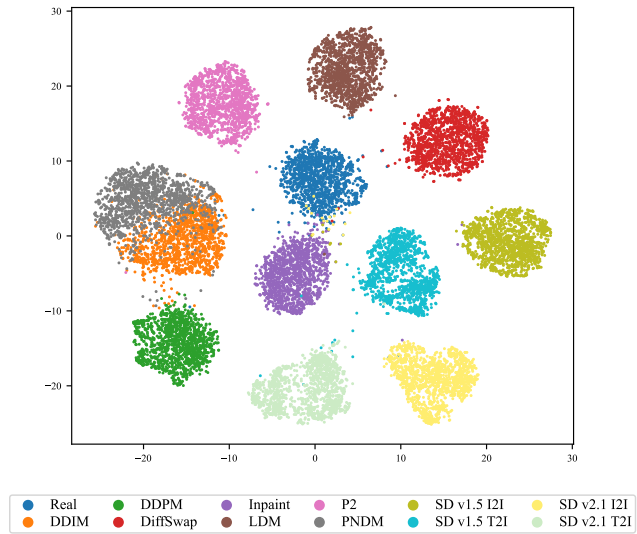
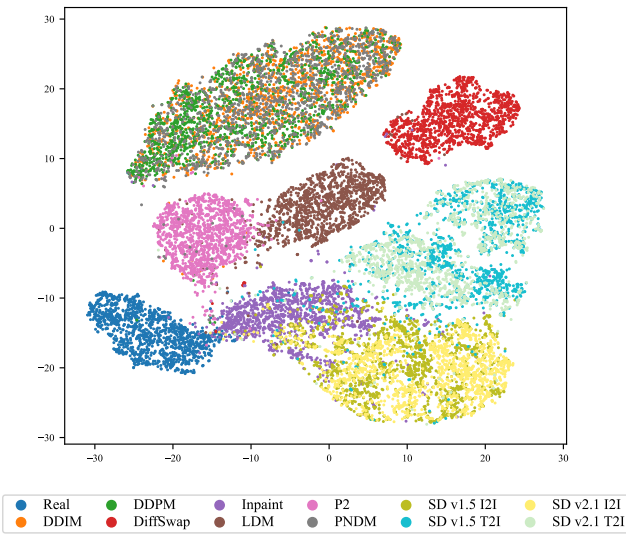


Figure 7. t-SNE feature visualization of various forgery face generators trained for binary classification.

Figure 8. t-SNE feature visualization of various forgery face generators trained for multiclass classification.

Train on	Unconditional Image Generation (Test Dataset)					Conditional Image Generation (Test Dataset)						Average Auc(%)
	DDPM	DDIM	PNDM	P2	LDM	SDv1.5 I2I	SDv1.5 T2I	SDv2.1 I2I	SDv2.1 T2I	Inpaint	DiffSwap	
DDPM	99.9	99.8	99.7	84.4	60.6	21.0	60.3	38.9	70.4	36.8	64.8	67.0
DDIM	99.5	99.9	99.9	90.2	56.5	23.0	55.6	29.7	71.9	38.9	76.3	67.4
PNDM	99.6	99.9	99.9	92.7	64.9	21.9	57.8	31.0	71.2	37.0	79.1	68.6
P2	76.9	97.8	98.0	99.8	99.7	51.3	95.1	60.7	83.9	38.8	93.2	81.4
LDM	31.6	52.6	54.1	83.9	99.9	72.2	88.0	75.7	69.0	50.5	81.1	69.0
SDv1.5 I2I	64.0	66.2	68.8	86.5	88.5	91.6	97.2	86.5	91.2	67.6	75.2	80.3
SDv1.5 T2I	64.5	80.9	78.6	82.1	93.5	84.5	99.9	77.5	99.7	58.9	72.1	81.1
SDv2.1 I2I	56.7	31.0	34.7	64.4	85.3	77.8	87.9	94.7	71.1	44.3	66.1	64.9
SDv2.1 T2I	89.4	92.4	91.0	78.3	84.3	79.8	99.3	70.1	99.9	67.7	68.6	83.7
Inpaint	39.7	19.8	21.7	39.2	44.0	99.6	46.5	40.3	35.2	99.8	43.4	48.1
DiffSwap	74.6	95.7	95.3	94.2	97.1	44.8	85.8	45.1	78.5	49.9	99.4	78.2

Table 8. Result of with-domain and cross-domain on different training and testing subsets using UniDetection.

Train on	Unconditional Image Generation (Test Dataset)					Conditional Image Generation (Test Dataset)						Average Auc(%)
	DDPM	DDIM	PNDM	P2	LDM	SDv1.5 I2I	SDv1.5 T2I	SDv2.1 I2I	SDv2.1 T2I	Inpaint	DiffSwap	
DDPM	99.9	99.9	99.9	83.8	57.1	39.2	30.9	57.1	35.7	49.8	64.7	65.3
DDIM	99.9	99.9	99.9	76.2	49.8	29.5	36.4	55.8	40.5	41.8	74.3	64.0
PNDM	99.9	99.9	99.9	83.7	58.7	37.3	45.8	60.5	50.3	47.2	69.9	68.5
P2	99.1	98.3	98.8	99.9	95.6	84.6	57.3	82.2	41.9	68.4	69.6	81.4
LDM	83.5	64.0	67.9	91.5	99.9	88.4	73.4	90.3	41.2	78.2	79.3	78.0
SDv1.5 I2I	57.2	67.0	68.2	55.6	80.0	100.0	99.3	88.8	92.9	94.6	47.5	77.4
SDv1.5 T2I	58.3	70.6	71.8	50.4	72.6	96.9	100.0	83.5	99.9	83.9	54.3	76.6
SDv2.1 I2I	81.1	83.1	83.3	80.5	84.9	99.6	96.7	99.9	97.2	86.6	69.0	87.4
SDv2.1 T2I	44.0	57.5	59.2	47.8	58.8	82.3	99.9	80.9	100.0	60.6	44.7	66.9
Inpaint	87.5	89.9	89.0	63.9	97.0	99.9	99.4	93.5	77.8	99.9	80.6	88.9
DiffSwap	71.0	72.3	72.2	59.9	78.8	51.6	59.6	63.3	40.0	63.0	99.9	66.5

Table 9. Result of with-domain and cross-domain on different training and testing subsets using SAIA.

depicted in Fig. 7. The detector achieves detection accuracies exceeding 98% across all categories. From the graph, we observe a convergence of features from several unconditional image generation methods (DDPM, DDIM, PNDM), while LDM and P2 remain distinct. In comparison to Text2Img, image-to-image methods exhibit a closer proximity to real images in the feature space, with Inpaint being the closest.

Multiclass classification Additionally, we visualize the feature space obtained through training the network for multiclass classification. In this scenario, the network distinguishes between various generation methods for each category, as depicted in Fig. 8. With known data for all categories, the forged categories are well-separated, with images generated by Inpaint and Image2Image methods partially blending with the real distribution.

9. More Visualization About DiffusionFace

We present additional visual examples from our dataset, encompassing both unconditional and conditional image generation. Unconditional image generation instances, featuring DDPM, DDIM, PNDM, P2, and LDM, are illustrated in

Fig. 9. Conditional image generation examples, showcasing Stable Diffusion Text2Img, Stable Diffusion Img2Img, Inpaint, DiffSwap, are displayed in Fig. 10, Fig. 11, Fig. 12, and Fig. 13 respectively. Additionally, images sourced from the internet are shown in Fig. 14.

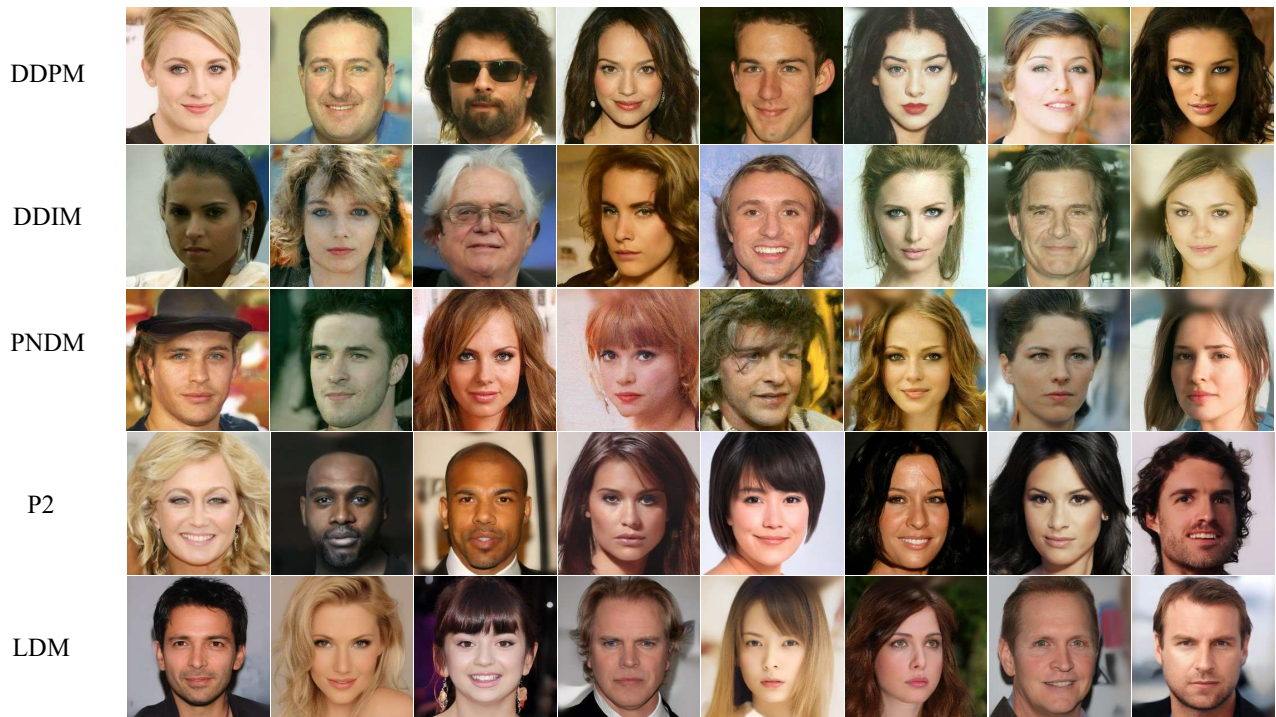


Figure 9. More visualization of Unconditional Image Generation, including DDPM, DDIM, PNDM, P2 and LDM.

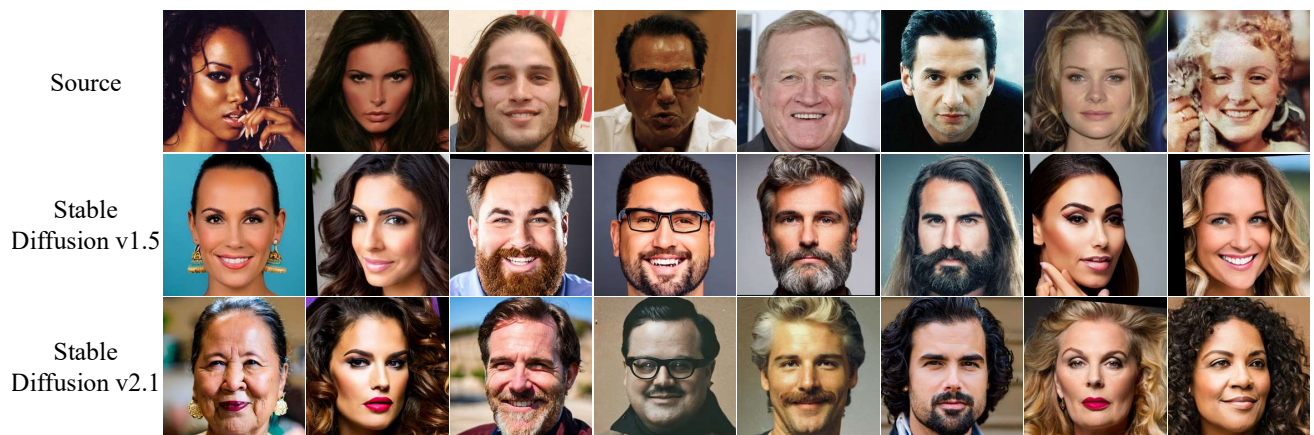


Figure 10. More visualization of Stable Diffusion Text2Image.



Figure 11. More Visualization of Stable Diffusion Image2Image.

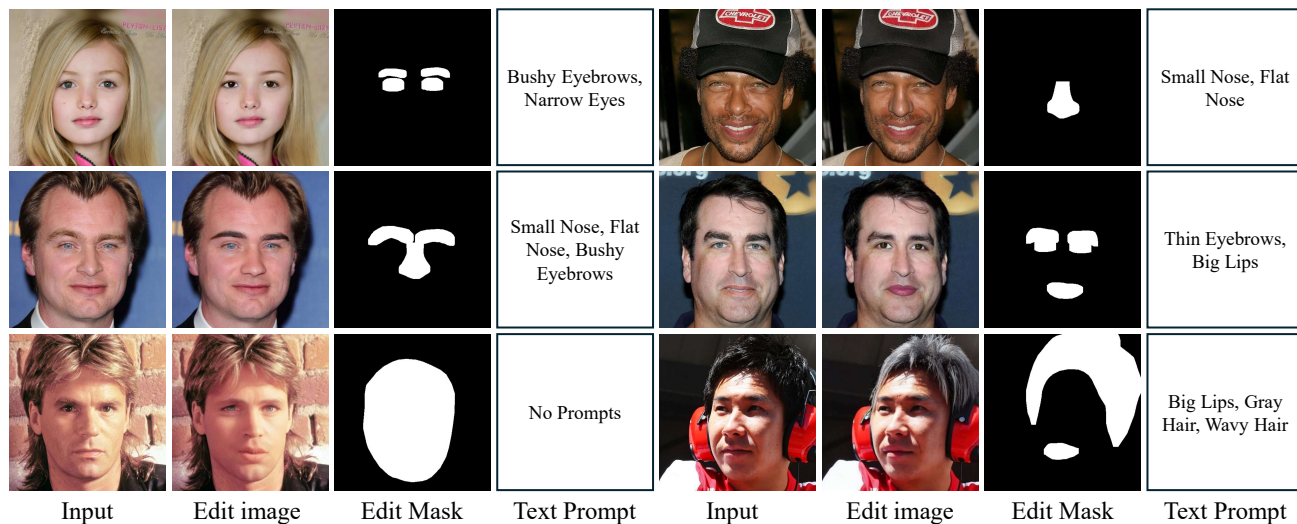


Figure 12. Visualization of Inpaint result.



Figure 13. More Visualization of DiffSwap.



Figure 14. More visualization of AI-generated face images sourced from the Internet.